Electronic Supplementary Material (ESI) for New Journal of Chemistry.

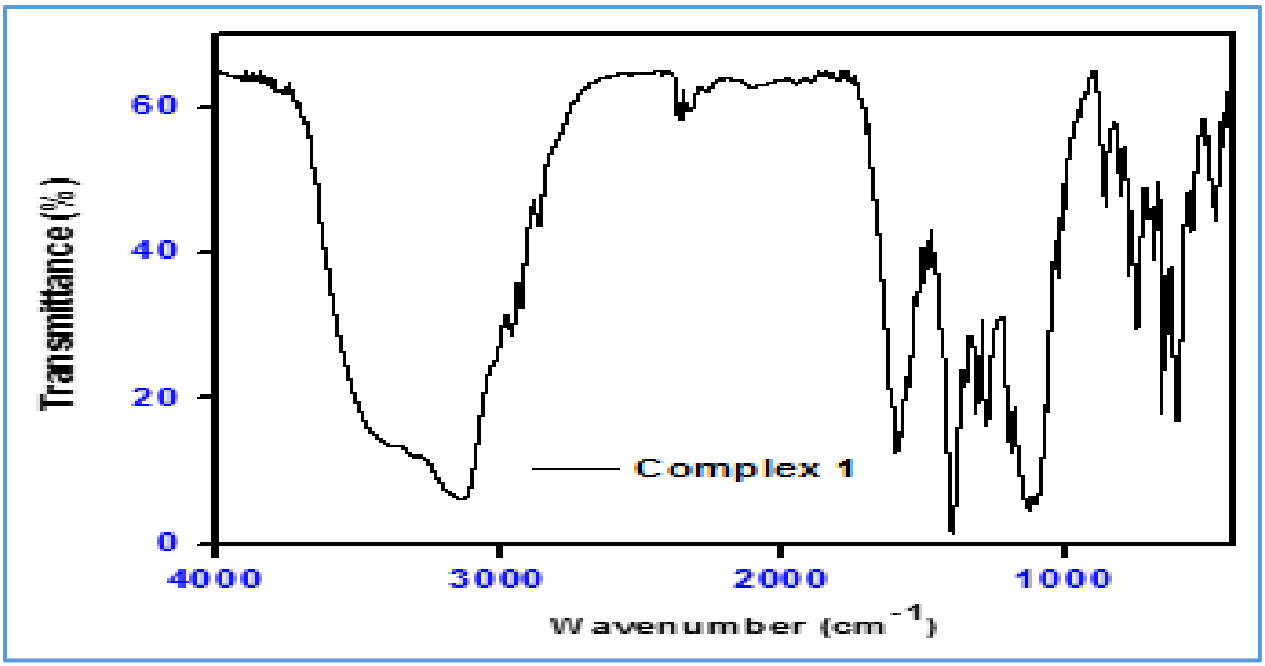

Figure S1: FT-IR spectrum of complex **1**.

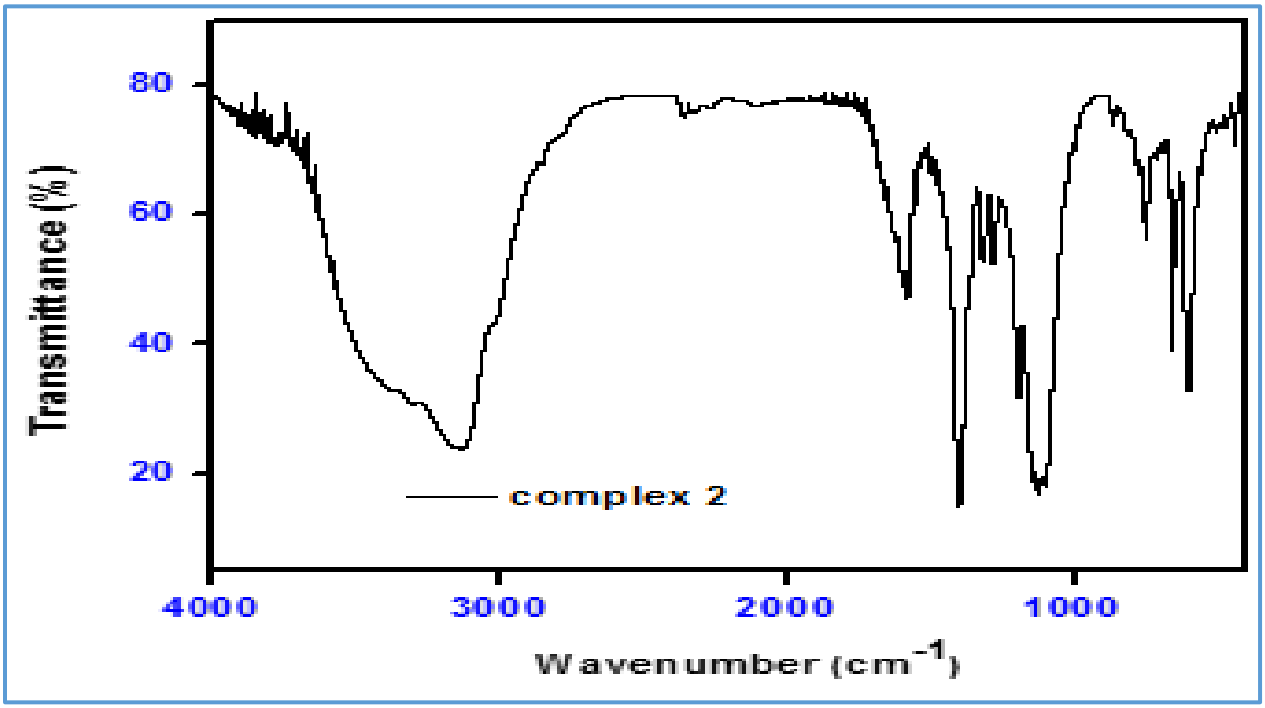

Figure S2: FT-IR spectrum of complex **2**.

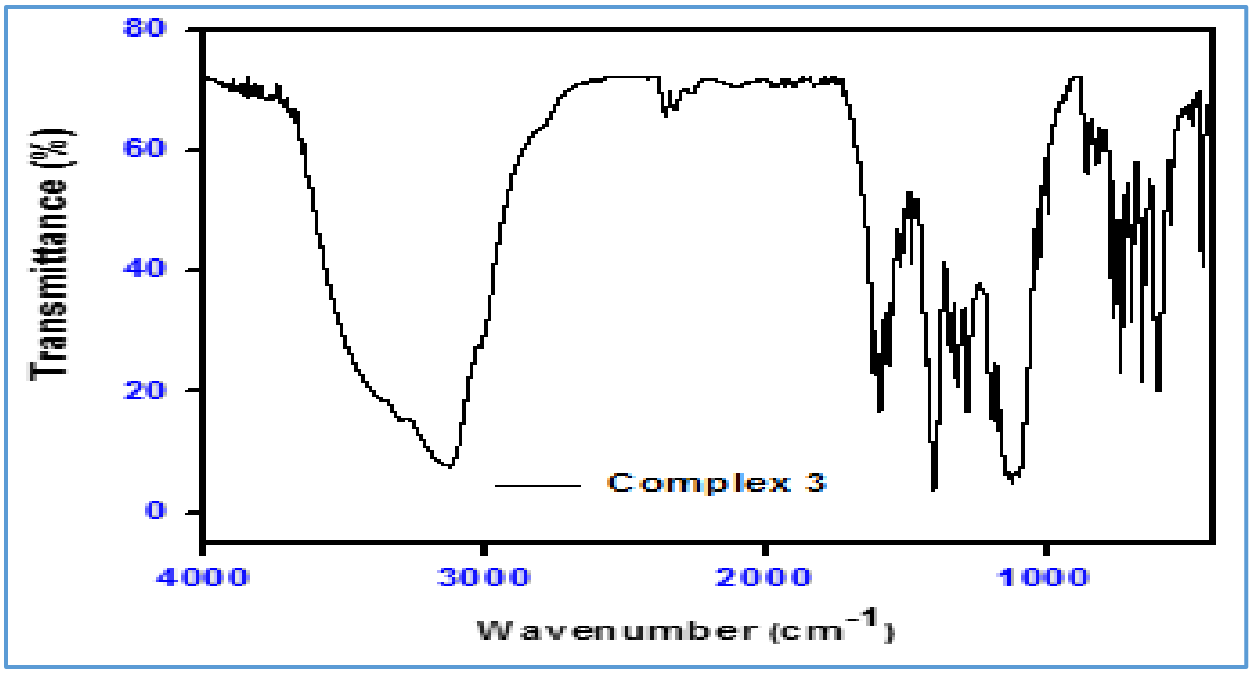

Figure S3: FT-IR spectrum of complex **3**.

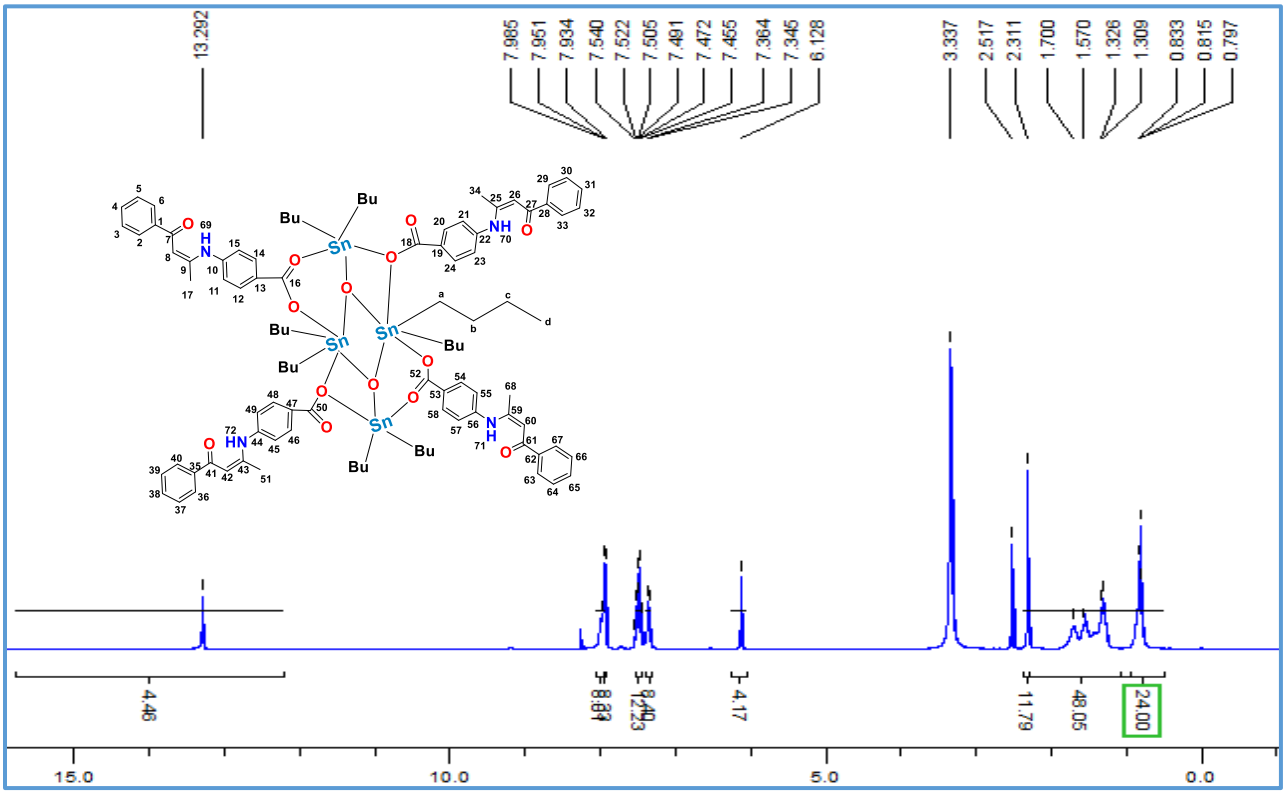

Figure S4: ^{1}H NMR spectrum of complex **1** recorded in ($CDCl_3$+ DMSO-d_6).

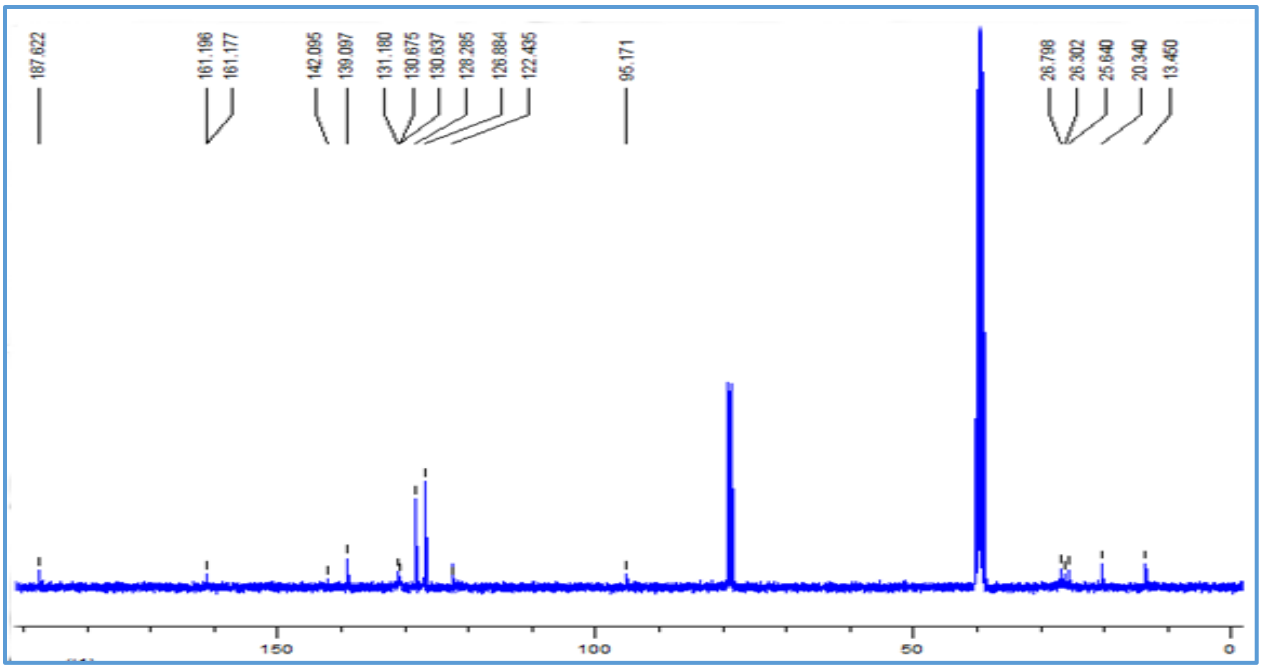

Figure S5: $^{13}C\{^{1}H\}$ NMR spectrum of complex **1** recorded in ($CDCl_3$+ DMSO-d_6).

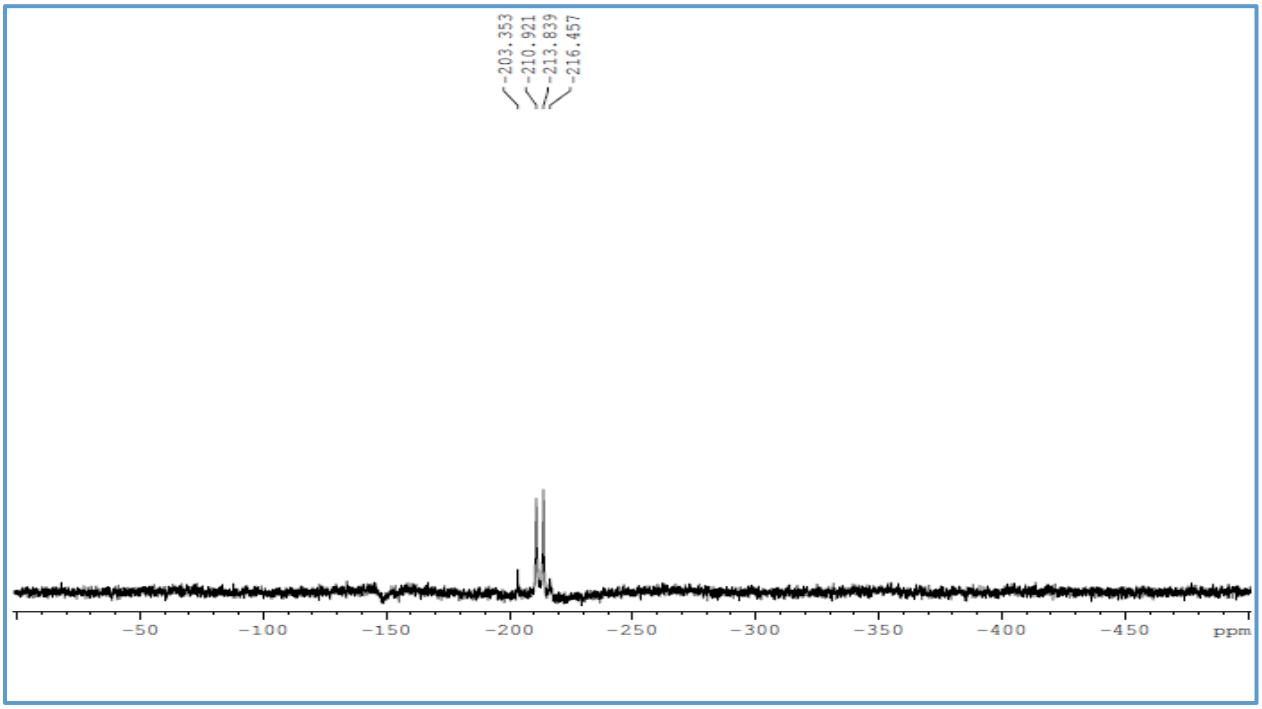

Figure S6: ^{119}Sn NMR spectrum of complex **1** recorded in $CDCl_3$.

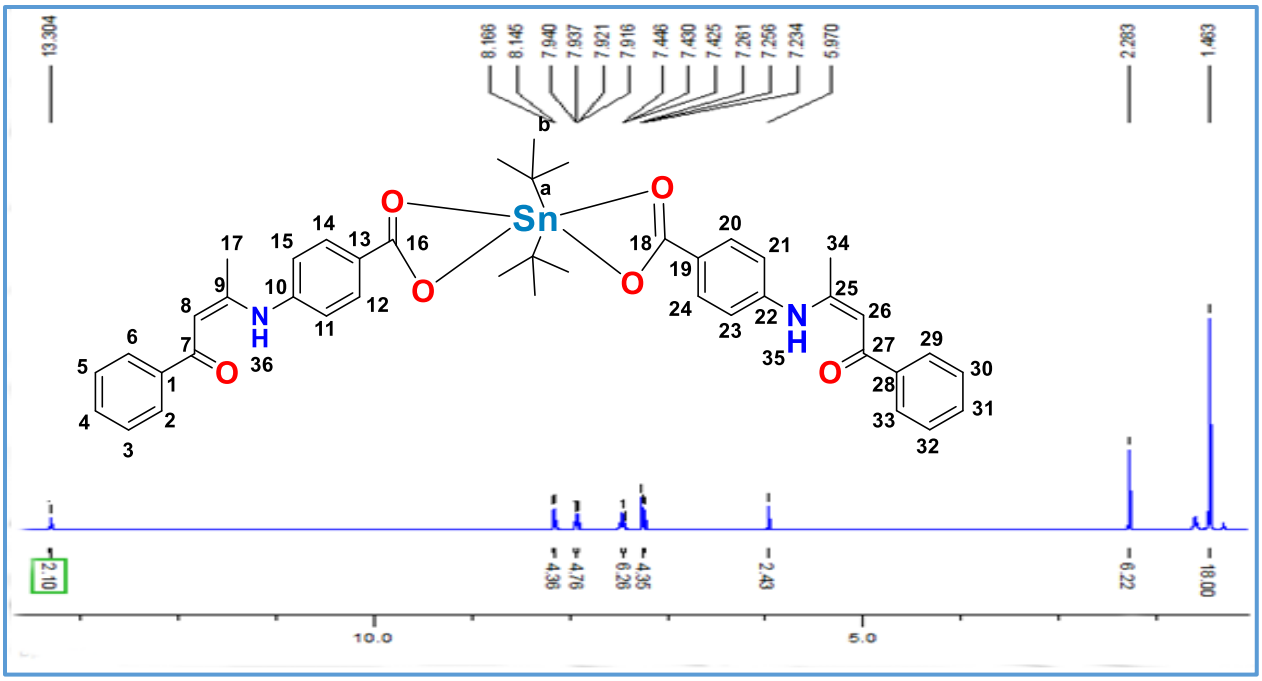

Figure S7: ^{1}H NMR spectrum of complex **2** recorded in $CDCl_3$.

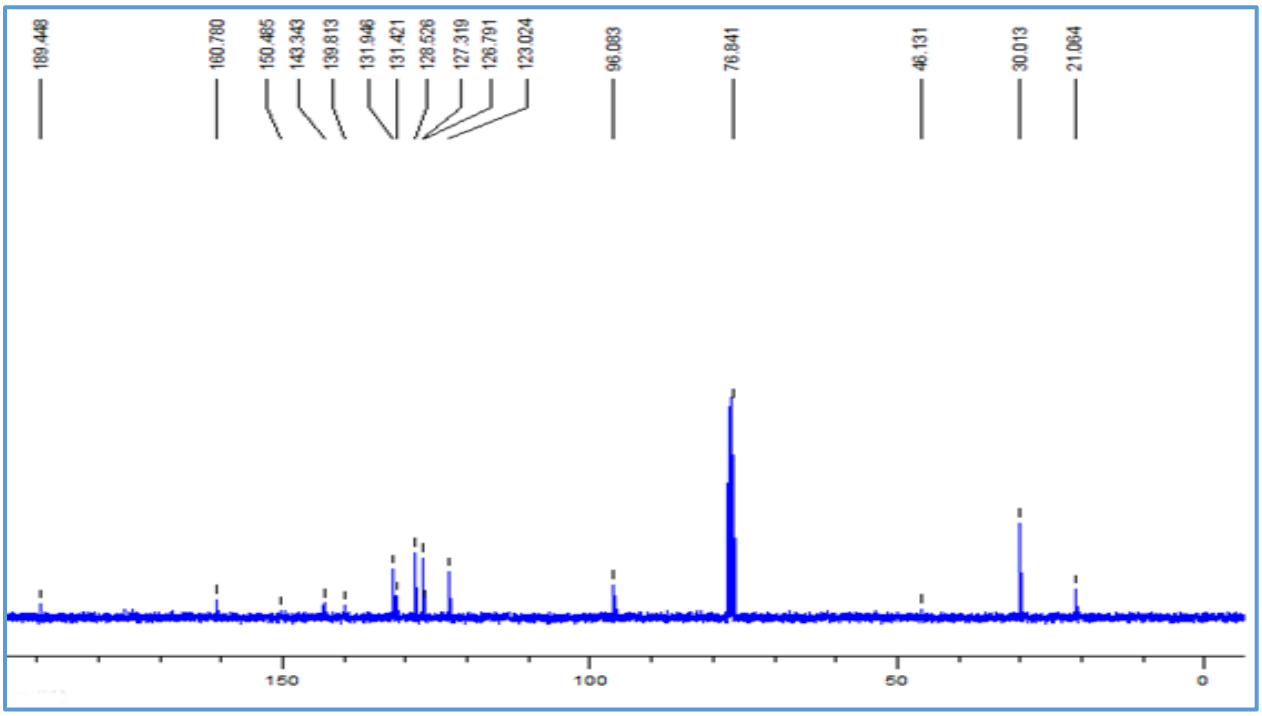

Figure S8: $^{13}C\{^{1}H\}$ NMR spectrum of complex **2** recorded in $CDCl_3$.

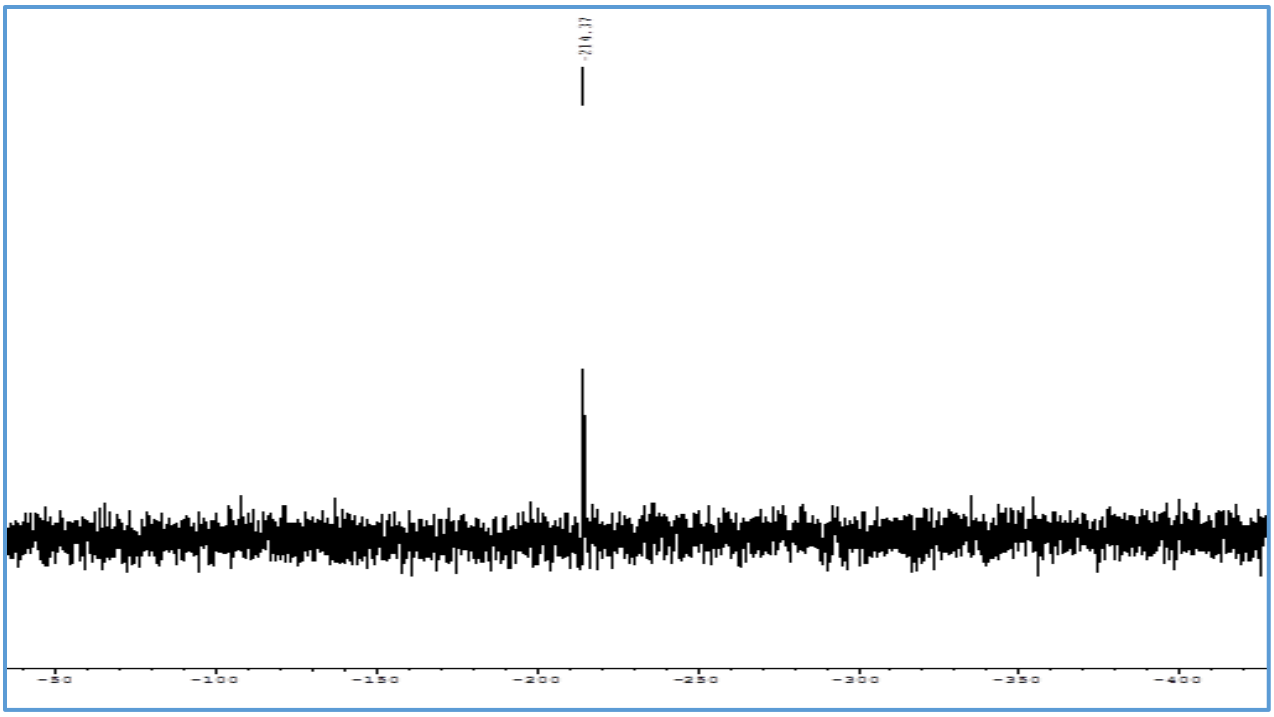

Figure S9: ^{119}Sn NMR spectrum of complex **2** recorded in $CDCl_3$.

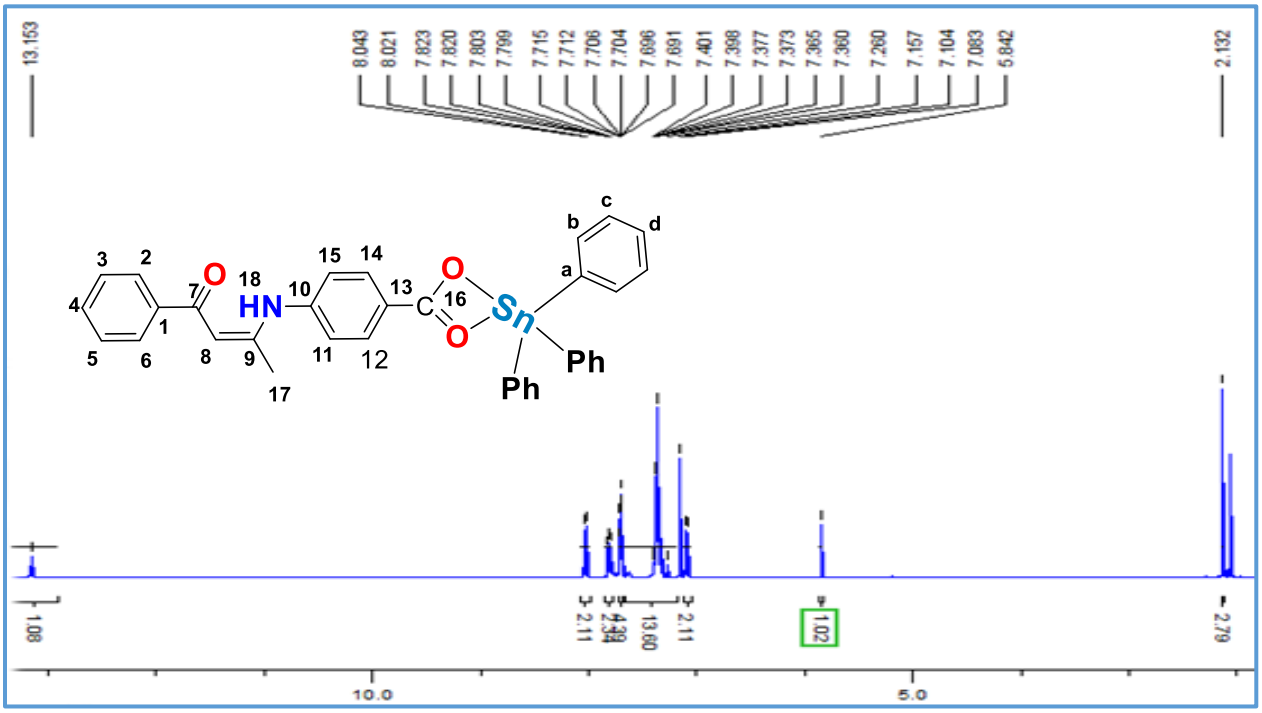

Figure S10: ^{1}H NMR spectrum of complex **3** recorded in $CDCl_3$.

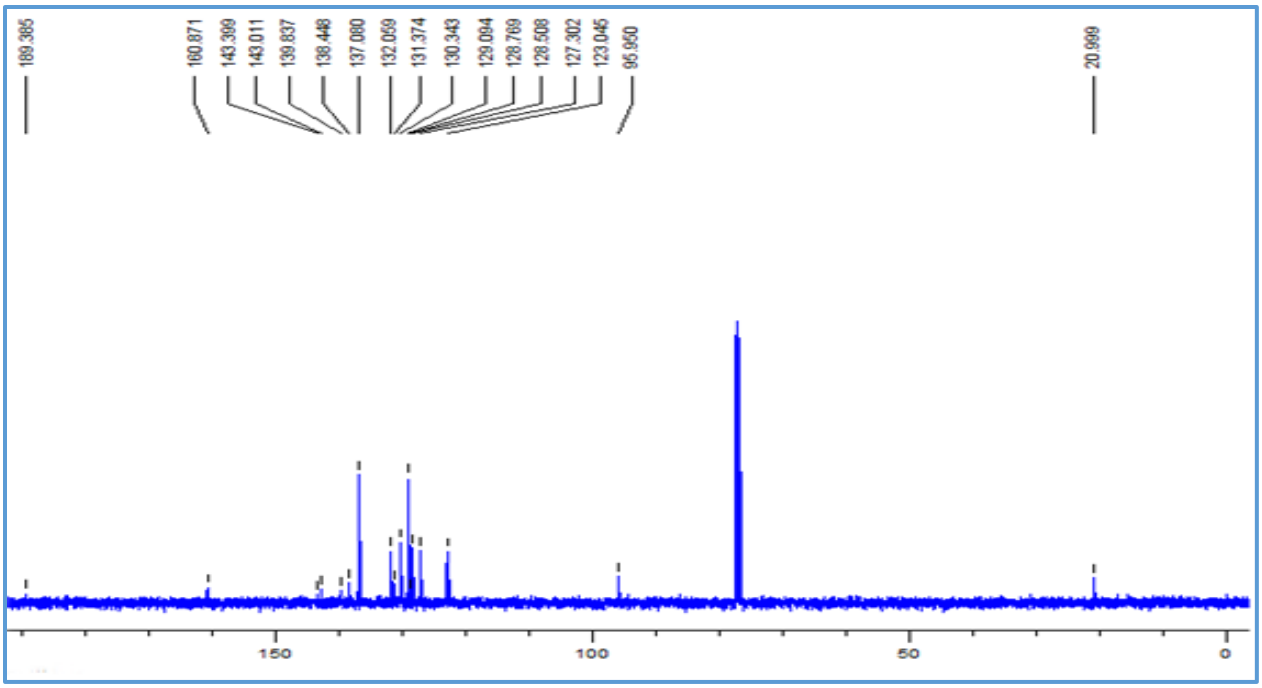

Figure S11: $^{13}C\{^{1}H\}$ NMR spectrum of complex **3** recorded in $CDCl_3$.

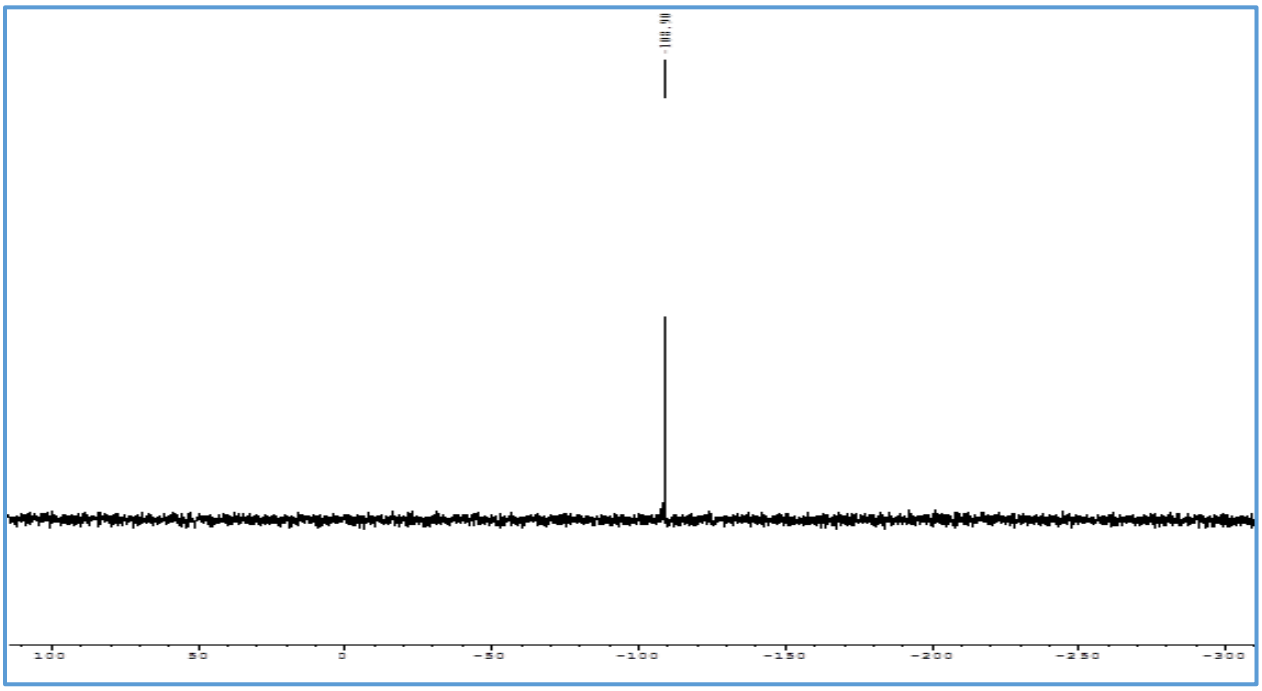

Figure S12: ^{119}Sn NMR spectrum of complex **3** recorded in $CDCl_3$.

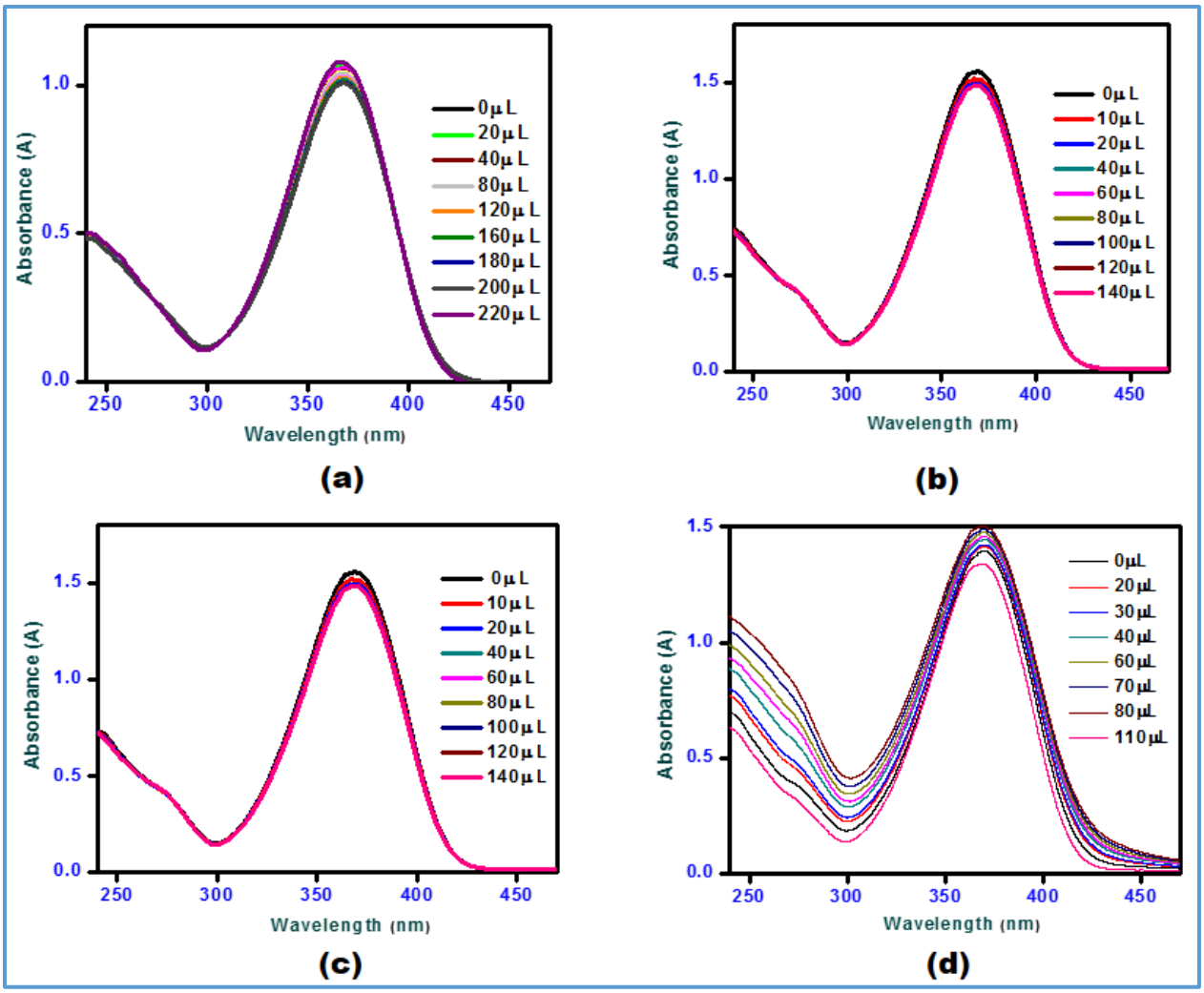

Figure S13: Absorption spectral variation of complex **1** (1.1 x 10^{-5} mol dm^{-3}) with the addition of 1-5 equivalent of nitrate salts (1.6 x 10^{-4} mol dm^{-3}) of **(a)** Ba^{2+} **(b)** Cr^{3+} **(c)** Co^{2+} **(d)** Fe^{3+} in methanol.

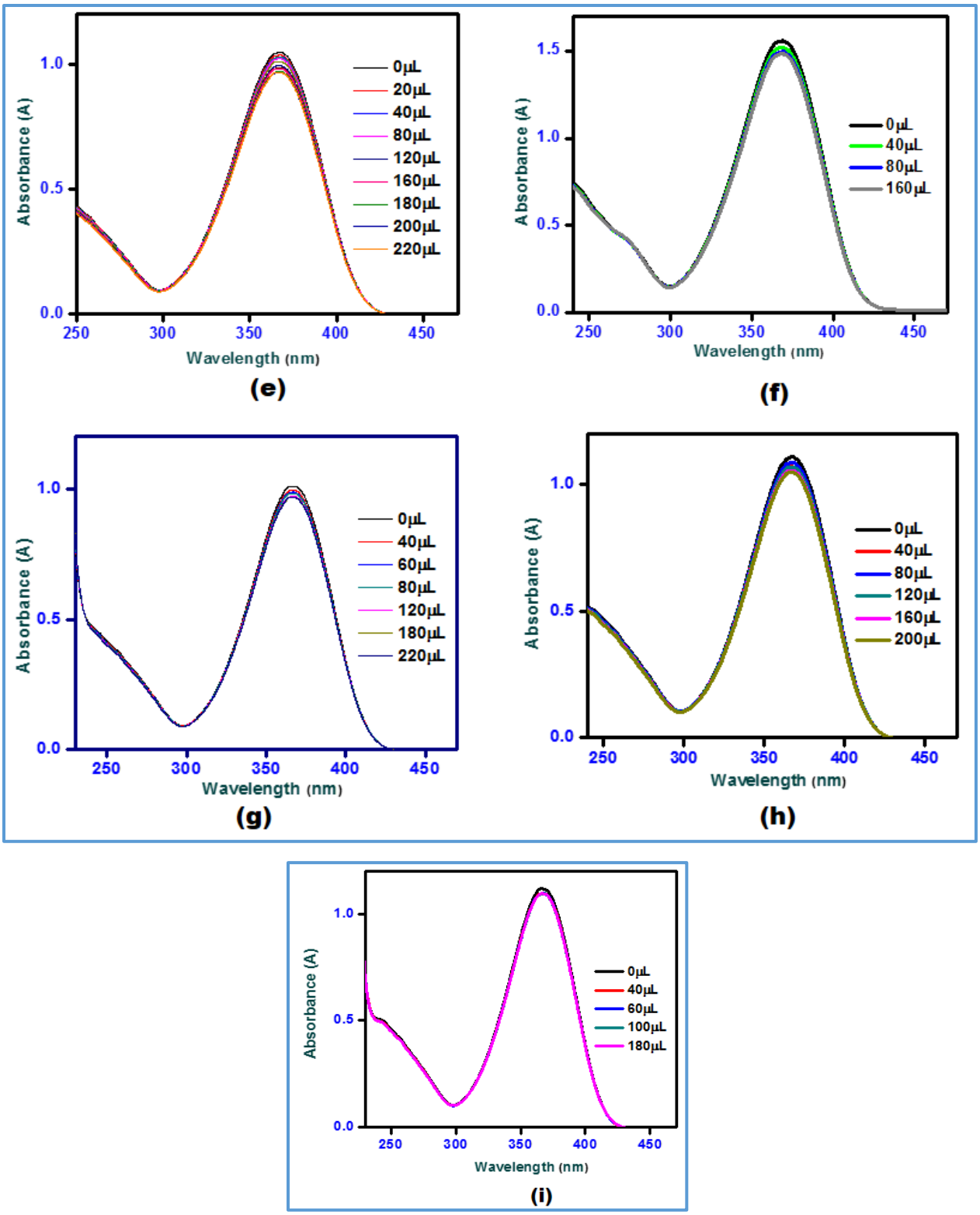

Figure S14: Absorption spectral variation of complex **1** (1.1 x 10^{-5} mol dm^{-3}) with the addition of 1-5 equivalent of nitrate salts (1.6x 10^{-4} mol dm^{-3}) of **(e)** Cd^{2+} **(f)** Mn^{2+} **(g)** Ni^{2+} **(h)** Ag^{+} **(i)** Zn^{2+} in methanol.

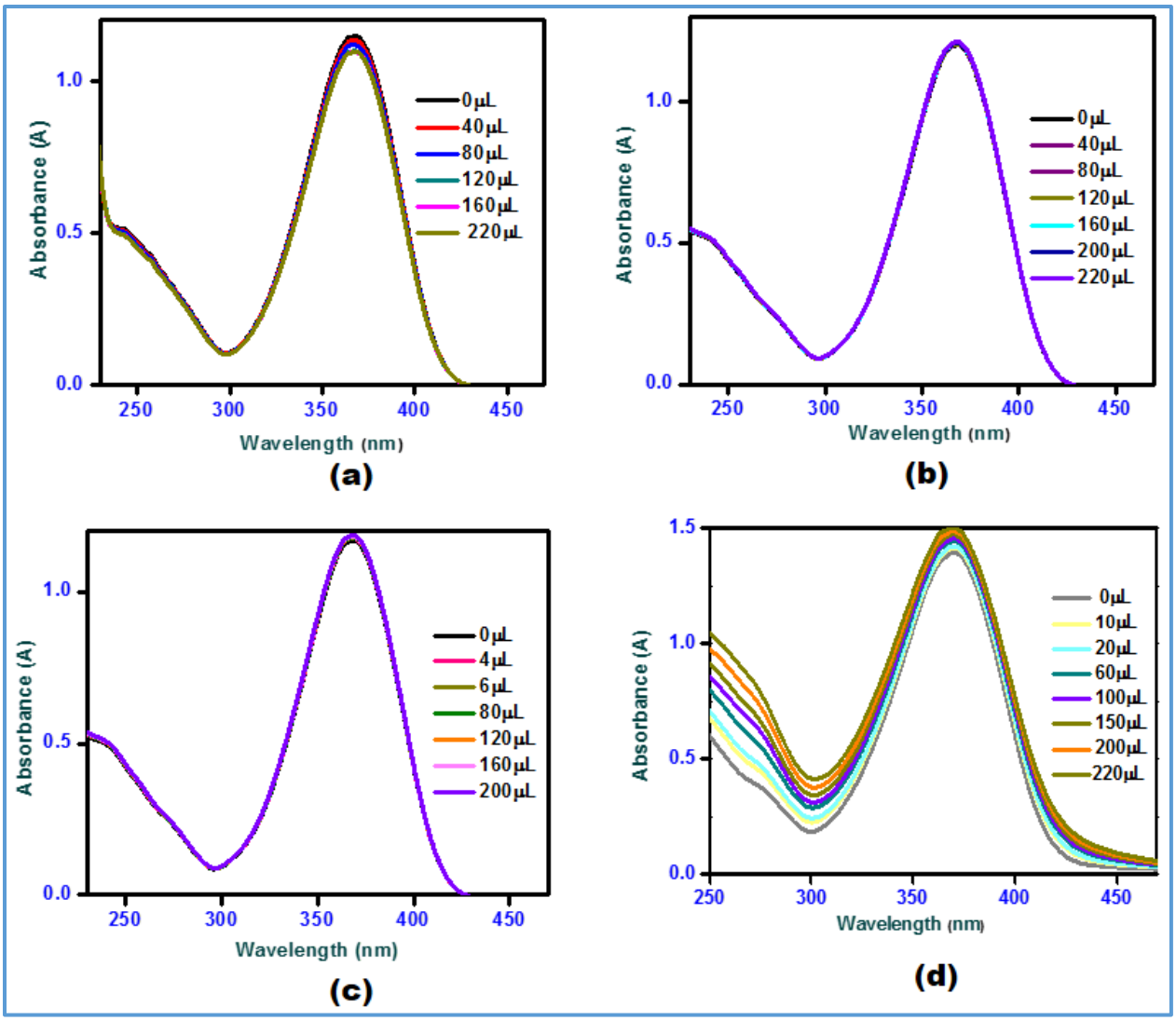

Figure S15: Absorption spectral variation of complex **2** (1.1 x 10^{-5} mol dm^{-3}) with the addition of 1-5 equivalent of nitrate salts (1.6 x 10^{-4} mol dm^{-3}) of **(a)** Ba^{2+} **(b)** Cr^{3+} **(c)** Co^{2+} **(d)** Fe^{3+} in methanol.

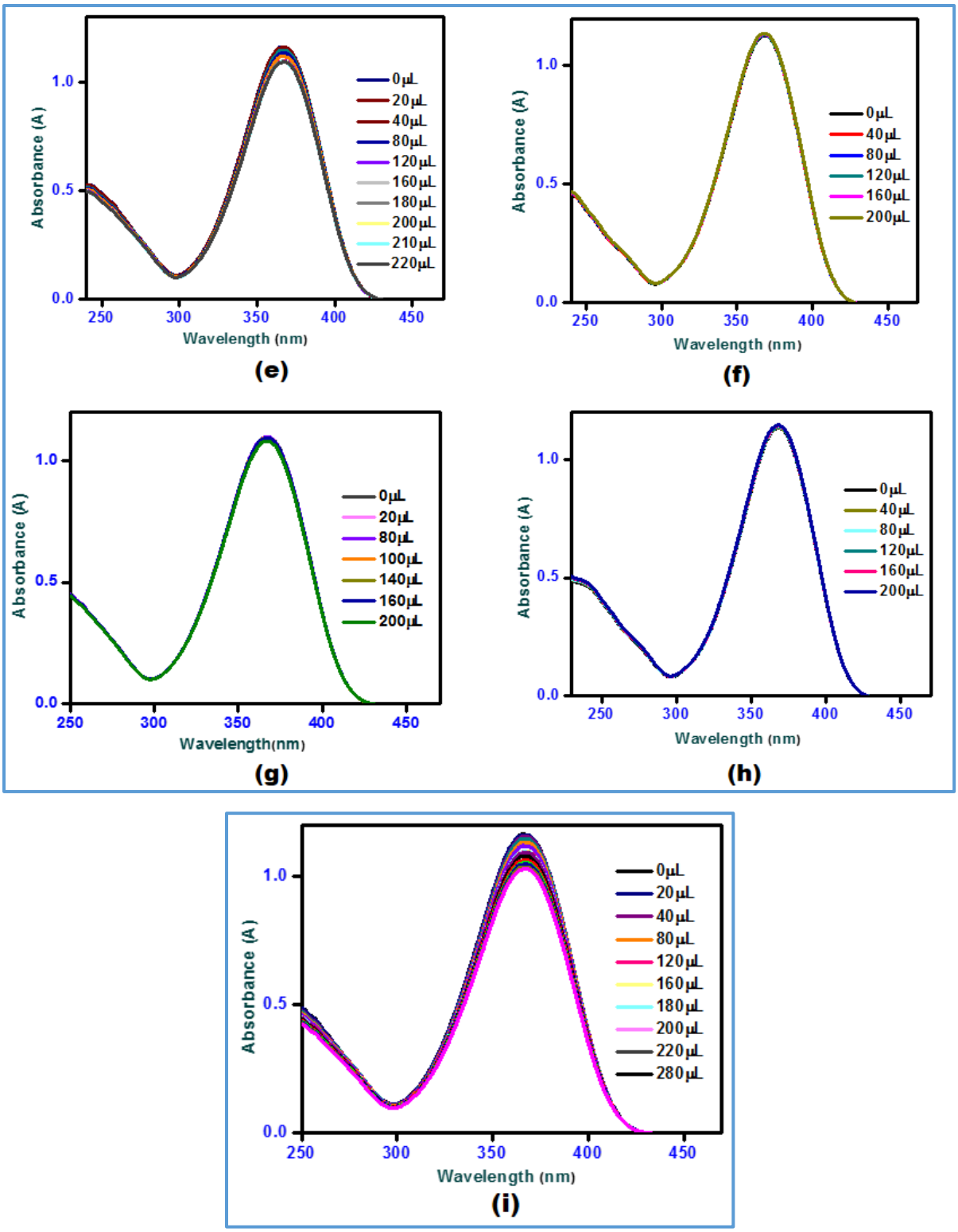

Figure S16: Absorption spectral variation of complex **2** (1.1 x 10^{-5} mol dm^{-3}) with the addition of 1-5 equivalent of nitrate salts (1.6x 10^{-4} mol dm^{-3}) of **(e)** Cd^{2+} **(f)** Mn^{2+} **(g)** Ni^{2+} **(h)** Ag^{+} **(i)** Zn^{2+} in methanol.

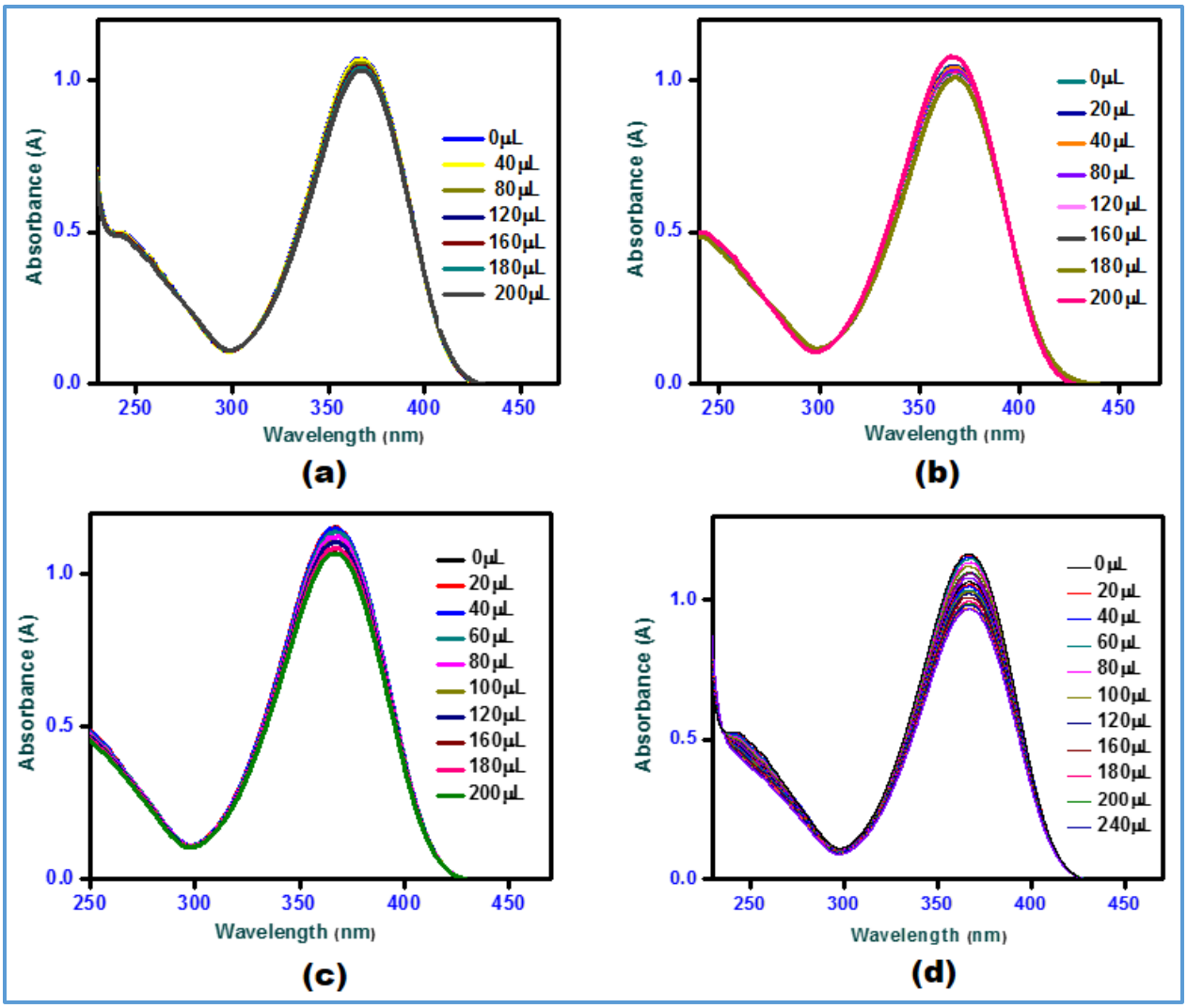

Figure S17: Absorption spectral variation of complex **3** (1.1 x 10^{-5} mol dm^{-3}) with the addition of 1-5 equivalent of nitrate salts (1.6 x 10^{-4} mol dm^{-3}) of **(a)** Ba^{2+} **(b)** Cr^{3+} **(c)** Co^{2+} **(d)** Fe^{3+} in methanol.

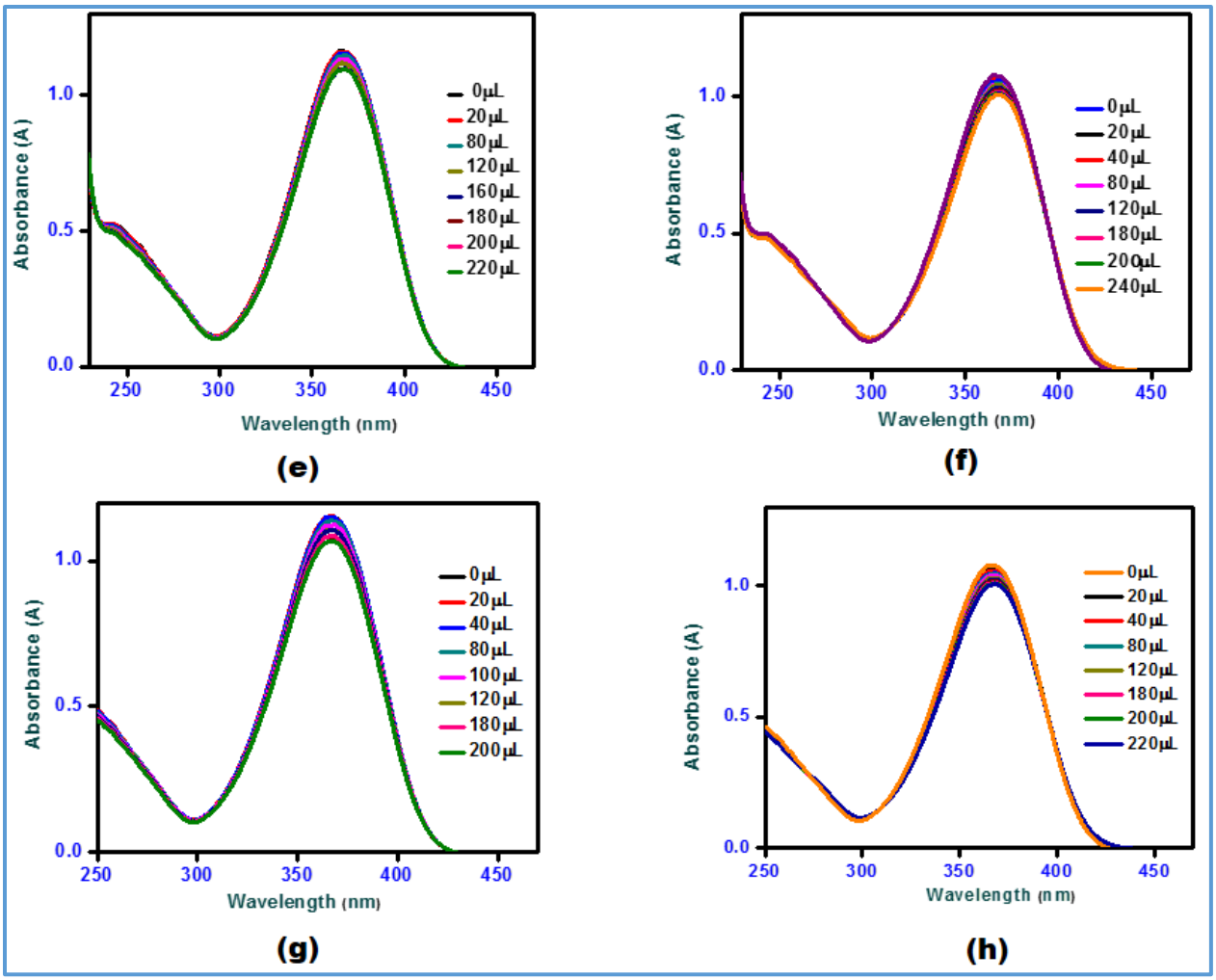

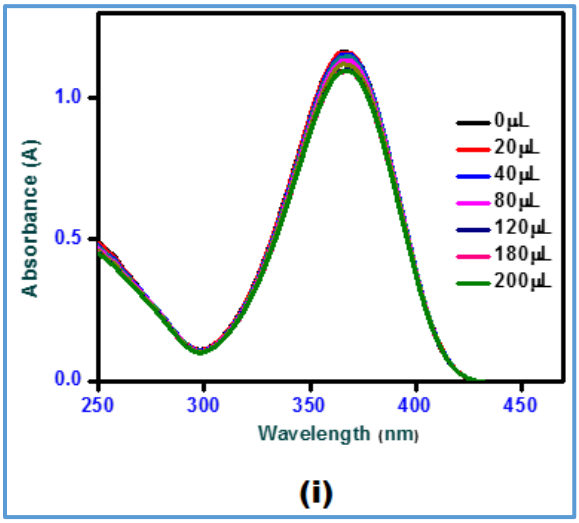

Figure S18: Absorption spectral variation of complex **3** (1.1 x 10^{-5} mol dm^{-3}) with the addition of 1-5 equivalent of nitrate salts (1.6x 10^{-4} mol dm^{-3}) of **(e)** Cd^{2+} **(f)** Mn^{2+} **(g)** Ni^{2+} **(h)** Ag^{+} **(i)** Zn^{2+} in methanol.

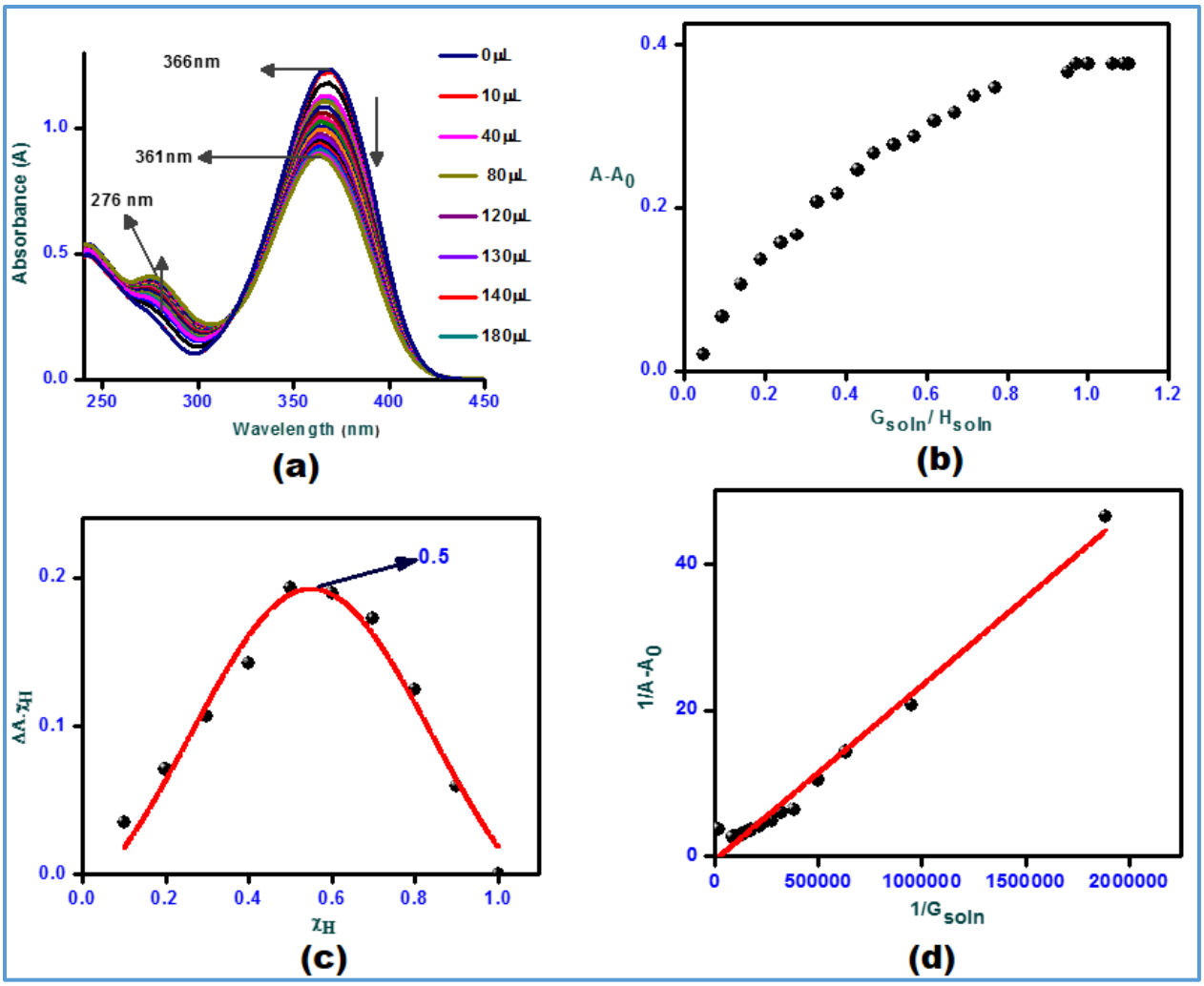

Figure S19: (a) Absorbance of complex **1** (1.1 x 10^{-5} mol dm^{-3}) with the addition of 1-5 equivalent of copper(II) nitrate trihydrate (1.6 x 10^{-4} mol dm^{-3}) in methanol. **(b)** Stoichiometric plot of complex **1** with copper(II) nitrate trihyate. **(c)** Job's plot of complex **1** with copper(II) nitrate trihydrate. (**d)** Benesi-Hildebrand plot of complex **1** with addition of copper(II) nitrate trihydrate.

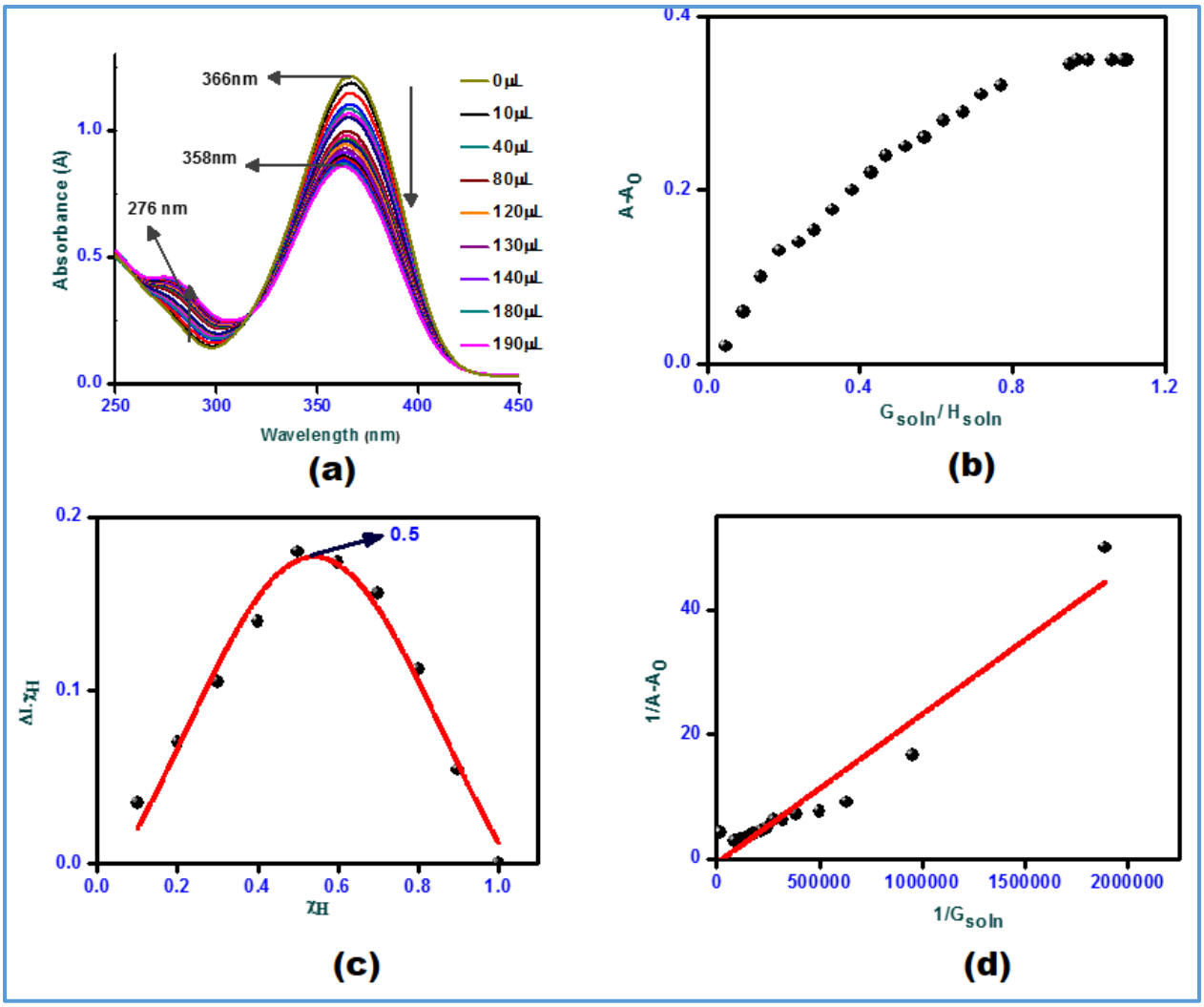

Figure S20: (a) Absorbance of complex **2** (1.1 x 10^{-5} mol dm^{-3}) with the addition of 1-5 equivalent of copper(II) nitrate trihydrate (1.6 x 10^{-4} mol dm^{-3}) in methanol. **(b)** Stoichiometric plot of complex **2** with copper(II) nitrate trihyate. **(c)** Job's plot of complex **2** with copper(II) nitrate trihydrate. (**d)** Benesi-Hildebrand plot of complex **2** with addition of copper(II) nitrate trihydrate.

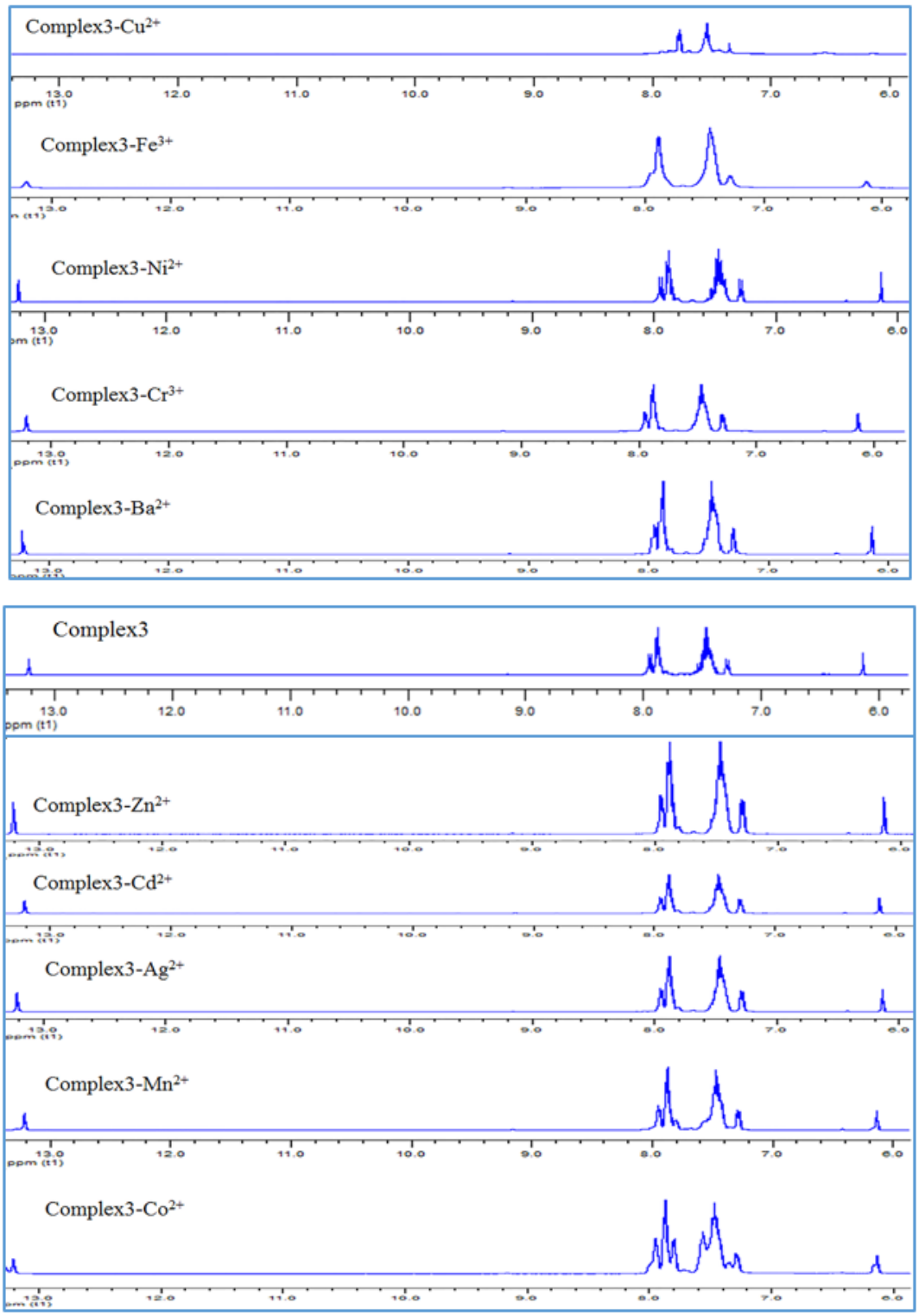

Figure S21: ^{1}H NMR spectra of complex **3** with the addition of an equivalent amount of selected metal ions in DMSO-d_6.

LOD (Limit of Detection) for complexes 1-3 with Cu^{2+} ion.

LOD for all complexes with Cu^{2+} ion was calculated from the absorption data. It was calculated by considering the band at wavelength 366 nm in all complexes **1-3** which gradually decreases on titration with 10 µL Cu^{2+} ion solution.

To determine the standard deviation for the absorbance, the absorbance of the individual receptors without any cation was measured by 15 times and the standard deviation of blank measurements was calculated.

The limit of detection (LOD) of the complexes for sensing of Cu^{2+} was determined from the following equation:

LOD = K × SD/S

Where K = 3 (according to IUPAC consideration); SD is the standard deviation of the blank receptor (complex **1-3**) solution; S is the slope of the calibration curve. From the linear fit of the graphs **S22**, **S23** and **S24**, slope (**S**) for all complexes are determined.

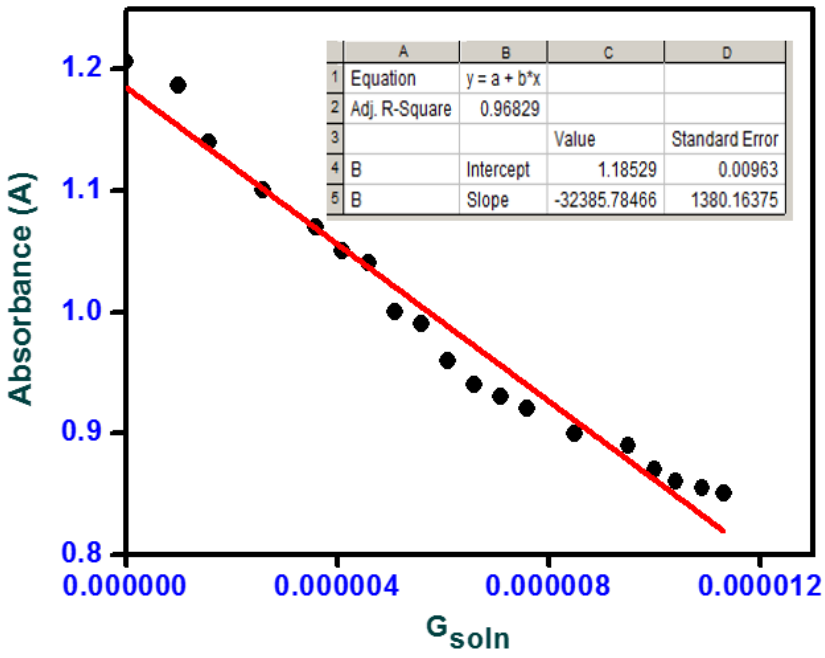

Figure S22: Graph between absorbance and concentration of guest (Cu^{2+}) for calculation of slope for complex **1**.

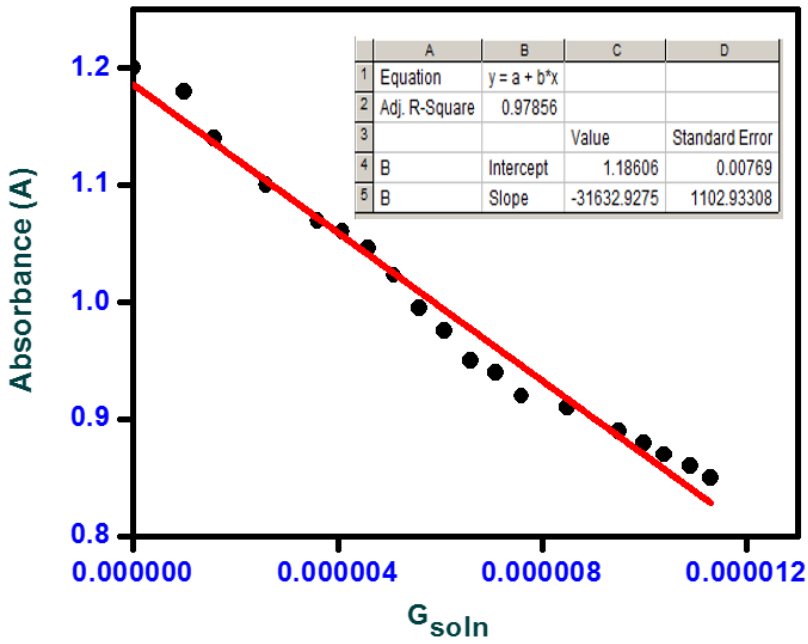

Figure S23: Graph between absorbance and concentration of guest (Cu^{2+}) for calculation of slope for complex **2**.

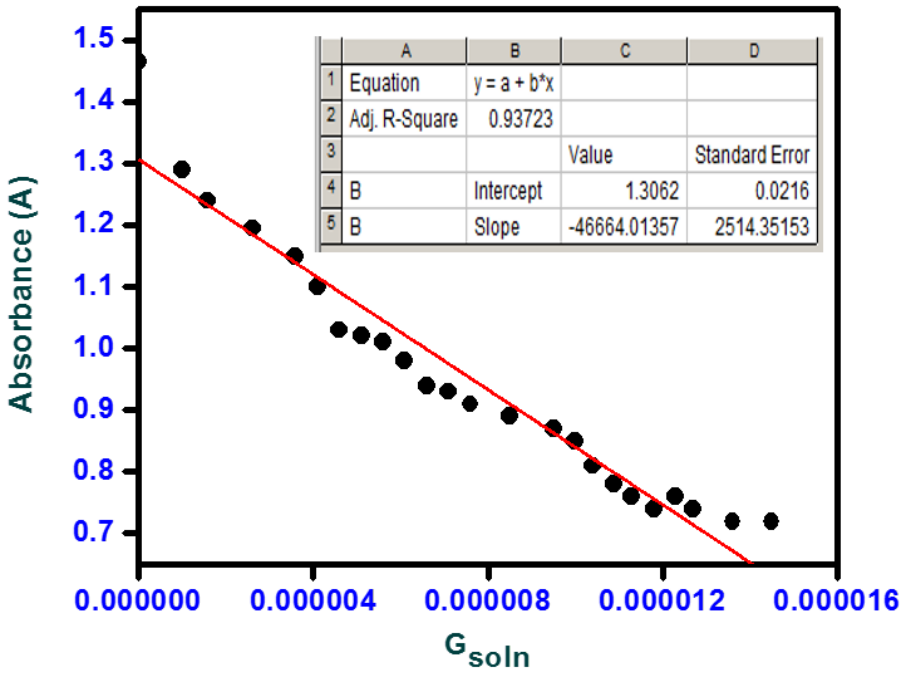

Figure S24: Graph between absorbance and concentration of guest (Cu^{2+}) for calculation of slope for complex **3**.

Complex **1**: K = 3; SD = 0.027 ; S = -32385.78; LOD = 2.5 $X10^{-6}$ M

Complex **2**: K = 3; SD = 0.028 ; S = -31632.92; LOD = 2.6 $X10^{-6}$ M

Complex **3**: K = 3; SD = 0.023 ; S = -46664.01; LOD = 1.47 $X10^{-6}$ M

The binding constant K can be calculated for complexes **1**-**3**.

we got intercept (C) and slope (m) value by linear fitting the graph (Benesi-Hildebrand plot) for complex **1**, **2** and **3** from plot **S19**(**d**), **S20**(**d**) and **3**(**d**) respectively.

K can be calculated by formula **C/m**.

Complex **1**: C = 0.477; m = 2.386 X 10^{-5} ; K = 0.19 X 10^{5} M^{-1}

Complex **2**: C = 0.631; m = 2.391 X 10^{-5} ; K = 0.26 X 10^{5} M^{-1}

Complex **3**: C = 0.433; m = 1.183 X 10^{-5} ; K = 0.40 X 10^{5} M^{-1}

X-ray crystallography

The intensity data of **1-3** were collected on a Rigaku SuperNova diffractometer equipped with an Eos S2 CCD detector, using MoKα radiation with graphite monochromator (λ = 0.71073 Å) at T = 293(2) K. The structure was solved by SHELXT and refined on F^2 by full-matrix least-squares methods using SHELXL using Olex2 as the graphical interface.[1-2] Non-hydrogen atoms were anisotropically refined. H-atoms were included in the refinement on calculated positions riding on their carrier atoms. The function minimized F_o^2) from counting statistics. The function R_1 and wR_2 were ($\sigma||F_o|$ - $|F_c||$) / $\sigma|F_o|$ and [σw (F_o^2 - F_c^2)^2 / $\sigma(wF_o^4)$]$^{1/2}$, respectively. Crystallographic data (excluding structure factors) for the structures reported in this paper have been deposited in the Cambridge Crystallographic Data Centre as a supplementary publication no. CCDC 1862874-1862876.

Copies of the data can be obtained free of charge on application to CCDC, 12 Union Road, Cambridge CB21EZ, UK (fax: + (44)1223-336-033; email: deposit@ccdc.cam.ac.uk

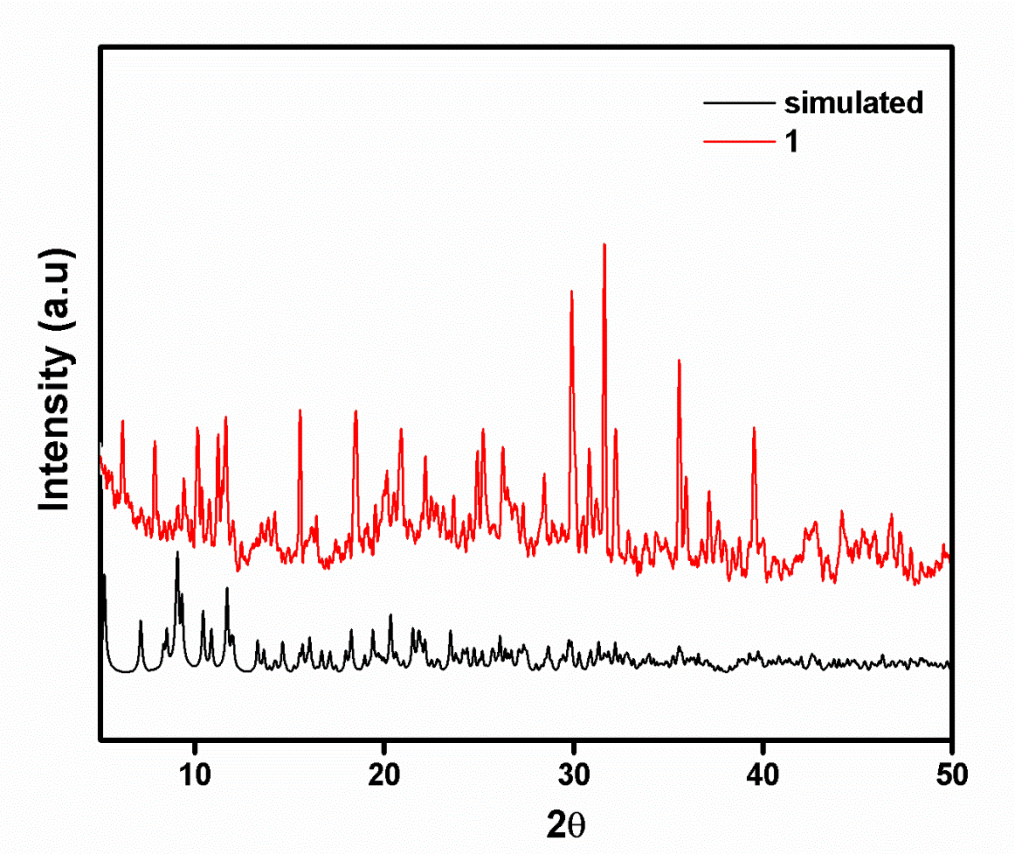

Figure S25: Powder XRD pattern of complex **1**.

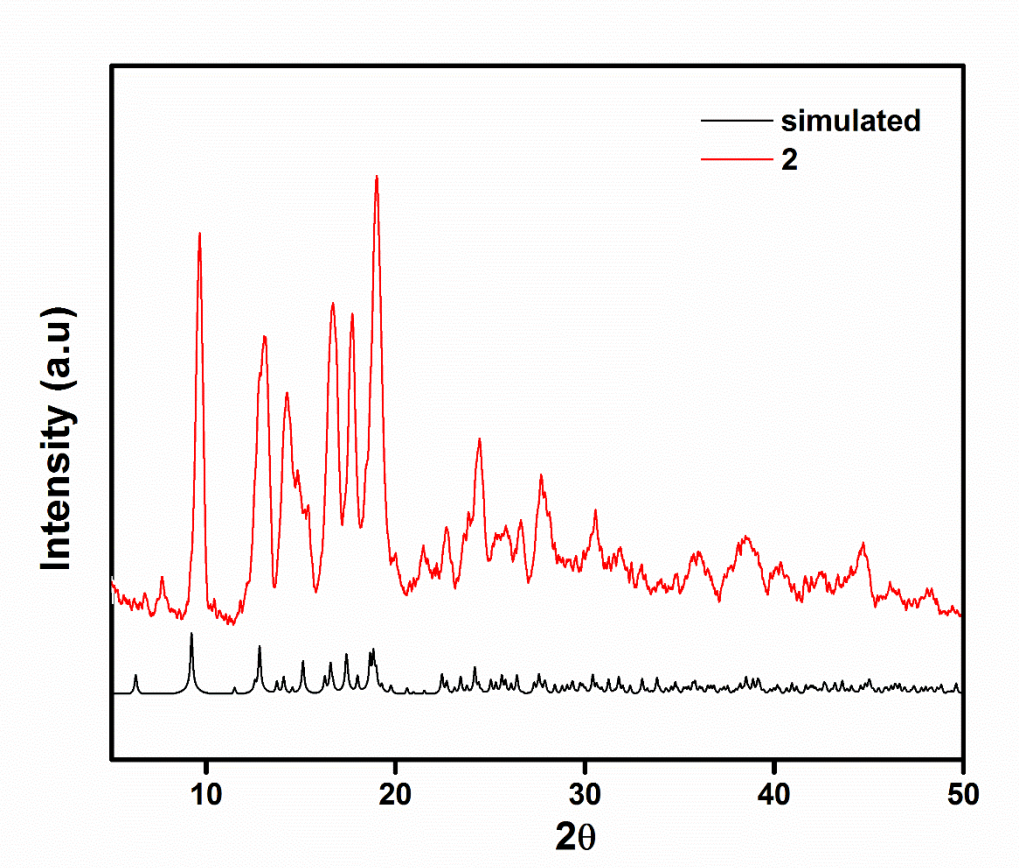

Figure S26: Powder XRD pattern of complex **2**.

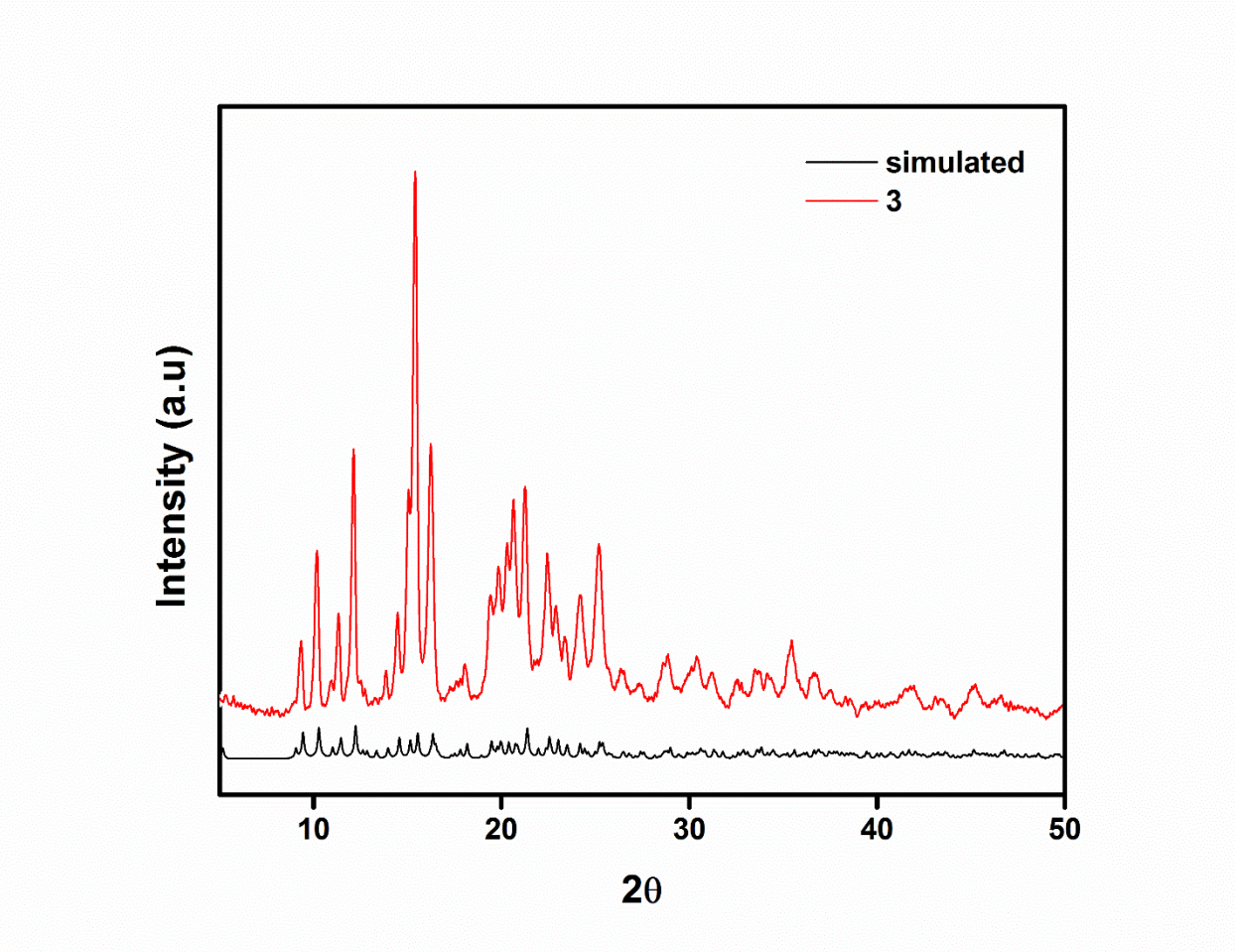

Figure S27: Powder XRD pattern of complex **3**.

References:

1. Sheldrick, G.M., Crystal structure refinement with ShelXL, *Acta Cryst.*, (2015), C71, 3-8.

2. O.V. Dolomanov and L.J. Bourhis and R.J. Gildea and J.A.K. Howard and H. Puschmann, Olex2: A complete structure solution, refinement and analysis program, *J. Appl. Cryst.*, (2009), **42**, 339-341.